Diagonal Discrete Hodge Operators for Simplicial Meshes Using the Signed Dual Complex

Ruben Specogna

Dipartimento di Ingegneria Elettrica, Gestionale e Meccanica, Università di Udine, Udine 33100, Italy

We present a technique to extend the geometric construction of diagonal discrete Hodge operators to arbitrary triangular and tetrahedral boundary conforming Delaunay meshes in the frequent case of piecewise uniform and isotropic material parameters. The technique is based on the novel concept of signed dual complex that originates from a physical argument. In particular, it is shown how the positive definiteness of the mass matrix obtained with the signed dual complex is easily ensured for all boundary conforming Delaunay meshes without requiring—as expected by the common knowledge—that each circumcenter has to lie inside the corresponding element. Eliminating this requirement, whose fulfillment presents otherwise formidable practical difficulties, enables one to easily obtain efficient, consistent, and stable schemes.

Index Terms—Diagonal discrete Hodge operator, finite integration technique (FIT), *M*-matrices, signed dual complex.

I. INTRODUCTION

IN THE last decade, there has been an increasing interest in reformulating physical laws directly in algebraic form. Finite integration technique (FIT) [1], cell method [2], generalized finite differences [3], discrete geometric approach [4], or discrete geometric methods [5] are instances of this philosophy. Global electromagnetic variables are associated to oriented geometric elements of a pair of dual grids in such a way that electromagnetic laws are naturally casted as exact topological equations. Constitutive laws are discretized by means of material matrices relating the introduced global variables.

The major advantage of geometric formulations is that, once the primal and dual grids are orthogonal, the resulting material matrices can be made diagonal. This represents a great asset for explicit Yee-like schemes [1], [6] to solve transient full-Maxwell problems and nowadays finite difference time domain-like codes are still leading the scene. We remark that also the solution of boundary value problems (BVPs) would benefit from such kind of material matrices, since they reduce the fill-in of the system matrix and produce *M*-matrices [7], that guarantee the discrete maximum principle preservation.

In literature, it is well-known that it is hard to extend the construction of diagonal material matrices to unstructured simplicial meshes. The dual node, which has to be placed in the circumcenter of the element to give rise to a pair of orthogonal grids, frequently lies outside the corresponding triangle (or tetrahedron). Many papers claim that this fact defeats any possibility to construct a consistent diagonal material matrix, see [5] and [8]–[12]. A triangulation such that each element contains its circumcenter, referred to as self-centered triangulation, is very hard to obtain for most practical problems. The proposed solutions to circumvent this issue, without pretending to be exhaustive, comprise techniques that give up the diagonality of the material matrices [11], [13] or by

techniques that do not even ensure consistency [5], [8], [14], yielding to less than first-order accurate schemes.

The aim of this contribution is to show that there exists a straightforward technique to construct diagonal, positive definite, and consistent material matrices for general boundary conforming Delaunay triangulations (CDTs), at least for piecewise uniform and isotropic materials.

This paper is organized as follows. Section II surveys, focusing on 2-D problems, the concept of boundary CDTs and presents a new recipe to compute the diagonal discrete Hodge operator. Section III generalizes the recipe to 3-D. Section IV shows the numerical results. Finally, conclusions are drawn in Section V.

II. 2-D PROBLEMS

Given a set of nodes in the plane in general position, the Delaunay triangulation is the unique triangulation such that the circumcircle of any element contains no node in its interior [15], see Fig. 1(a) and (b). Not all triangulations are Delaunay, but it has been proved in [16] that the Delaunay triangulation can be found after a series of local edge swaps consisting of substituting a pair of triangles with a new pair sharing the same nodes, but having different edges, Fig. 1(c). In computational engineering, one usually needs to represent the polygons that describe the boundary of the triangulation, which is not always convex, and internal interfaces between different materials. This is performed by requiring the triangulation to use a list of edges that represent such boundaries.

We focus on a narrower class of Delaunay triangulations, the boundary CDTs [17], [18]. Apart from the Delaunay condition, a CDT requires also that the diametral circle of every boundary edge have not to contain other nodes of the triangulation. The CDT are important since they have the virtue to guarantee that the circumcircles of all triangles lie inside the triangulation [18], Fig. 2(a). To construct a CDT, it is in general necessary to add some nodes on boundary edges to make sure that the aforementioned constraint is fulfilled, Fig. 2(b). It can be proved that this refinement on boundary edges suffices to obtain a CDT [17], [18]. Contrarily to self-centered triangulations, which are very hard to obtain, mesh generators as triangle [19] produce a CDT for any
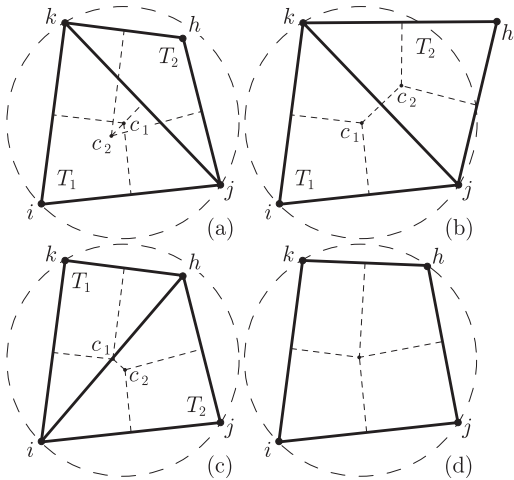
Fig. 1. (a) Two triangles T_1 and T_2 that do not satisfy the Delaunay condition (node h is inside the circumcircle of T_1). This dual complex is not valid since it does not partition the domain. (b) Two triangles T_1 and T_2 that satisfy the Delaunay condition and are self-centered. (c) By applying an edge swap to configuration (a), the two triangles now satisfy the Delaunay condition. This example illustrates how not all Delaunay triangulations are self-centered. (d) Degenerate case when four nodes lie on a circumference. This case is solved by perturbing the nodes or by creating a quadrilateral element.
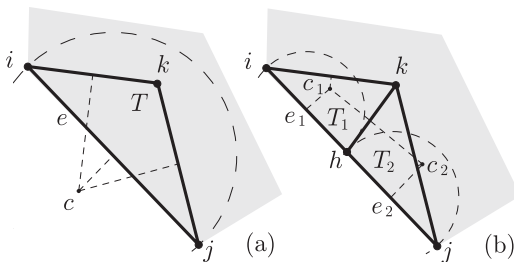

Fig. 2. (a) Triangle T in the boundary of the triangulation sketched in gray. Diametral circle of the boundary edge e contains a node of the triangulation (i.e., k) and circumcenter c lies outside the triangulation. Therefore, e should be refined to obtain a CDT triangulation. (b) After adding one node h that refines edge e in two edges e_1 and e_2, the diametral circles of e_1 and e_2 do not contain other nodes and circumcenters c_1 and c_2 of triangles T_1 and T_2 lie inside the triangulation.

input geometry with theoretical bounds on the time and nodes required [17], [18].

If the nodes of triangles are in general position, a Delaunay mesh is dual to the Voronoï mesh [15], [20]. Dual nodes are defined as the circumcenters of triangles. The straight dual edges connect pairs of dual nodes relative to triangles sharing an edge. On the boundary, dual edges are open and it is customary to add a dual mesh on the boundary to impose boundary conditions [2]. Since the Voronoï diagram is a partition of the input geometry into convex polygons [20], dual edges are always non-self-intersecting and their lengths are positive. Example of dual meshes for Delaunay or non-Delaunay triangulations are shown in Fig. 1(a)–(c). It should be noted, however, that the Delaunay condition does not guarantee that the mesh is self-centered [16]. In computational electromagnetics literature, the construction of diagonal Hodge operators is considered unfeasible for meshes as the one in Fig. 1(c), see [5] and [8]–[12]. This paper extends the construction of diagonal Hodge operators from self-centered meshes to CDT.
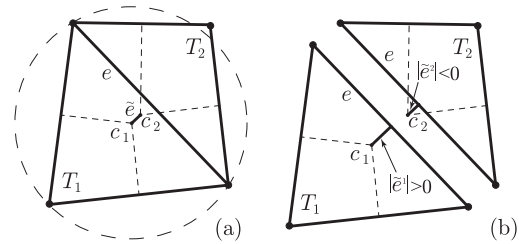

Fig. 3. (a) Dual edge $\tilde{e}$ dual to edge e is the segment having c_1 and c_2 as boundary. (b) It is convenient to compute the length of $\tilde{e}$ by mimicking the element-wise finite element assembly. In (a), the portion of $\tilde{e}$ in T_1 has a positive length, whereas the one inside T_2 has a negative length. By summing up the two lengths, we recover the length of $\tilde{e}$.

Before going further, we remark that there exists a degenerate case when the Delaunay–Voronoï duality is missing. This happens when four or more nodes lie on a circumference, Fig. 1(d). In this case, the Delaunay triangulation is not unique (all possible triangulations that split the quadrangle satisfy the Delaunay condition) and the interior dual edges have zero length. Even if probabilistically the chance of picking even just four nodes on a circle is near zero (since the circle has zero measure in $\mathbb{R}^2$), this case is classically solved by applying a perturbation on the input nodes to reduce again to the general case. An alternative solution is to merge all involved triangles to create a more complicated cell, as the quadrilateral element in Fig. 1(d).

A. Diagonal Material Matrix for 2-D Problems

We now introduce a simple way to assemble the diagonal material matrix $\mathbf{M}^\rho$ element by element, as usually performed in finite elements and differently from classical FIT [1]. That is, for each element T_i, we assemble at position (e, e) of $\mathbf{M}^\rho$ the following contribution for each edge e in T_i:

$$\mathbf{M}_{e,e}^\rho = \mathbf{M}_{e,e}^\rho + \rho \, \frac{|\tilde{e}^i|}{|e|} \tag{1}$$

where $|\tilde{e}^i|$ is the signed length of the portion inside T_i of dual edge $\tilde{e}$ dual to e, ρ is the uniform material parameter in T_i, and $|e|$ the length of e. The line passing through e divides the plane into two half-planes. We put a negative sign to $|\tilde{e}^i|$ if the circumcenter c_i is on a different half-plane with respect to the node of T_i not incident to e. For an enlightening example Fig. 3(b). It should be now clear why, to guarantee positive entries in the diagonal material matrix, it is essential for the mesh to be a CDT. Then, the consistency and positive definiteness of the whole material matrix follow immediately.

III. 3-D PROBLEMS

We described in detail the 2-D case, because pictures and concepts are easier to understand and especially because most of what is described for 2-D problems can be generalized to 3-D. For example, the Delaunay condition requires each circumsphere of any element to contain no node in its interior. In addition, the Voronoï diagram is still a partition of the input geometry into convex polygons [20], which implies that dual edges (dual faces) are always non-self-interesting and their lengths (areas) are positive. In 3-D, Delaunay–Voronoï

duality is lost: 1) when a circumcenter is equidistant to five or more nodes and 2) when four or more nodes lie on a circumference. Both cases are solved either by perturbation or as performed in Fig. 1(d). A CDT, analogously to 2-D, requires that the Delaunay property to hold also for boundary faces and edges. Unfortunately, available mesh generators as TETGEN [21] can generate a CDT with a guaranteed upper bound on the number of generated nodes only if the angle between any two surfaces describing the input geometry is bigger than 60°. Yet, there are algorithms such as [22]–[25] that do not have such requirements on input geometry, but they are hard to code and no available implementation exist. Even if more research about CDT generation is needed to cover this gap, currently a CDT can be generated for most practical problems.

A. Diagonal Material Matrices for 3-D Problems

The material matrix $\mathbf{M}^\rho$ that maps degrees of freedom (DoF) associated to faces to the ones associated with dual edges can be formed as in (1). That is, for each element T_i, we assemble the following contribution for each face f of T_i:

$$\mathbf{M}^\rho_{f,f} = \mathbf{M}^\rho_{f,f} + \rho \frac{|\tilde{e}^i|}{|f|} \tag{2}$$

where $|\tilde{e}^i|$ is the signed length of the portion inside T_i of dual edge $\tilde{e}$ dual to f, ρ is the uniform material parameter in T_i, and $|f|$ the area of f. The plane in which f lies divides the space into two half-spaces. We put a negative sign to $|\tilde{e}^i|$ if the circumcenter c_i is on a different half-space with respect to the node of T_i not incident to f.

In 3-D, there is also the material matrix $\mathbf{M}^\sigma$ that maps DoFs associated to edges to the ones associated with dual faces. To find its entries, for each element T_i, we assemble the following contribution for each edge e of T_i:

$$\mathbf{M}^\sigma_{e,e} = \mathbf{M}^\sigma_{e,e} + \sigma \frac{|\tilde{f}^i|}{|e|} \tag{3}$$

where $|\tilde{f}^i|$ is the signed area of the portion inside T_i of dual face $\tilde{f}$ dual to e, σ is the uniform material parameter in T_i, and $|e|$ the length of e. The $|\tilde{f}^i|$ is the sum of two triangles. Let us find the sign to the one whose vertices are the circumcenter c_i, the edge midpoint E, and the circumcenter F of face f (the two possible $f \in T_i$ that give rise to the two triangles are the ones having e in their boundaries), Fig. 4(a). The plane in which f lies divides the space into two half-spaces. In addition, also the line passing through e divides the plane in which f lies into two half-planes. Fig. 4(a)–(d) shows the four possible configurations and the relative signs to use.

IV. NUMERICAL RESULTS

Major benefits of the proposed technique are obtained in explicit Yee-like schemes for solving transient electromagnetic propagation. On the contrary, in this paper, we explore advantages in solving Poisson-like BVPs formulated as [26]

$$\mathbf{D}\mathbf{M}^{-1}_\rho\mathbf{D}^T\tilde{\mathbf{V}} = \mathbf{D}\mathbf{M}^{-1}_\rho\tilde{\mathbf{U}}_s \tag{4}$$
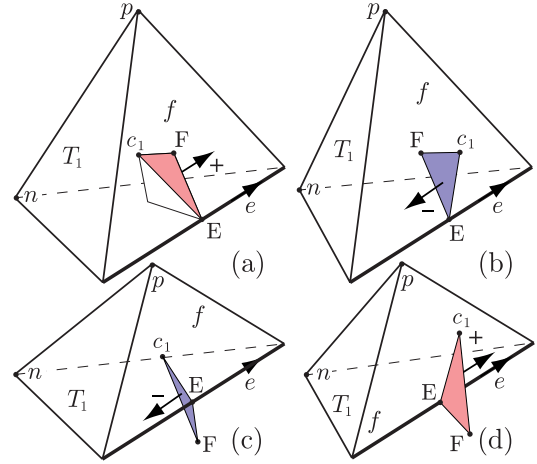

Fig. 4. (a) Sign is positive when c_1 is in the same half-space as node n and F is in the same half-plane as node p. (b) Sign is negative when c_1 is in the opposite half-space as n and F is in the same half-plane as p. (c) Sign is negative when c_1 is in the same half-space as n and F is in the opposite half-plane as p. (d) Sign is positive when c_1 is in the opposite half-space as n and F is in the opposite half-plane as p.
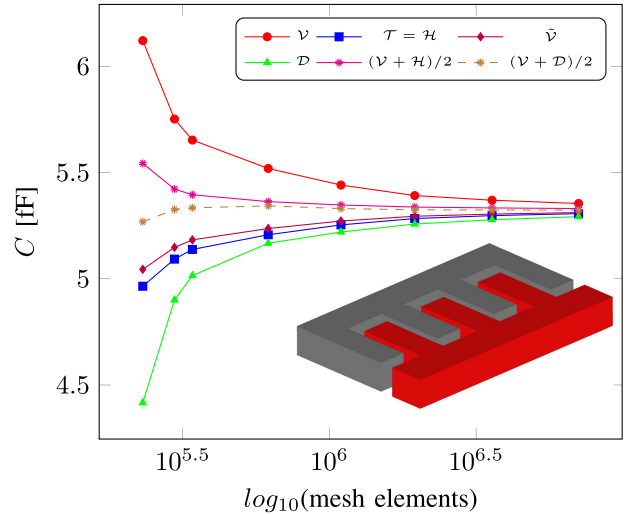

Fig. 5. Geometry of the MEMS comb drive and convergence of the capacitance with adaptive mesh refinement.

where $\mathbf{D}$ contains the incidences between elements-faces pairs, $\tilde{\mathbf{V}}$ contains the unknown scalar potential on dual nodes, and $\tilde{\mathbf{U}}_s$ is a known electromotive force used to impose Dirichlet boundary conditions. We compare this formulation $\mathcal{D}$ in terms of accuracy and simulation time with other four formulations surveyed in [26]: 1) the finite elements formulation $\mathcal{V}$ based on the scalar potential; 2) the formulation $\mathcal{T}$ based on the vector potential; 3) the geometric mixed-hybrid formulation $\mathcal{H}$; and 4) the $\tilde{\mathcal{V}}$ based on a sparse construction of dual Hodge operators.

First, it has been verified that the $\mathcal{D}$ formulation fulfills the piecewise uniform current density patch test consisting of a planar resistor fed by electrodes placed at two parallel planes of a cube. The resistor is made of two materials of resistivity 1 and 100 Ωm such that the interface between them is parallel to the electrodes and divides the resistor in half. Even though there are >23% of a total of 1701 tetrahedra
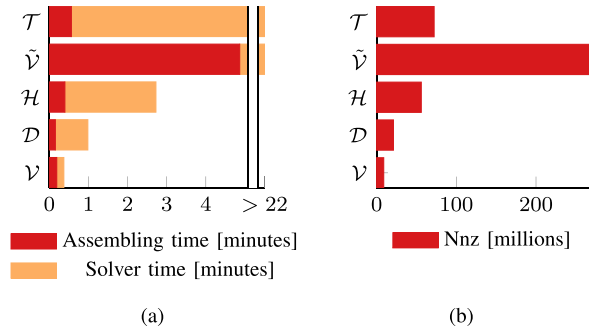
Fig. 6. (a) Simulation time for the MEMS comb drive problem on the finest mesh (∼7.1 millions tetrahedra, 1.2 millions nodes). $\tilde{\mathcal{V}}$ and $\mathcal{T}$ formulations need 23 and 38 min, respectively. (b) Number of non-zero entries of the sparse matrix.

whose circumcenters are outside them, as expected the solution is correct up to machine precision.

A further code validation is performed by verifying the convergence of the resistance of a square resistor [26] with an increasing number of elements (there is no room to show the results here). We present the results on a more complicated benchmark proposed in [5], which comprises a micro electro-mechanical system (MEMS) comb drive placed on a ground plane. For this problem, [5] considers diagonal material matrices technically unfeasible. On the contrary, the technique proposed in this paper produces consistent and symmetric and positive definite diagonal material matrices for all meshes, even though they are adaptively generated and always >30% of elements have circumcenters outside them. Fig. 5 compares how the capacitance computed by the various techniques converges when the number of elements is adaptively increased. Fig. 6(a) and (b) shows the time required and the number of non-zero elements in the system matrix for each formulation.

V. Conclusion

This paper claims the prerequisites that a simplicial mesh must fulfill to construct diagonal Hodge operators (i.e., diagonal material matrices) for problems involving isotropic materials. Delaunay triangulations, in fact, are necessary but not sufficient for the purpose, whereas self-centered triangulations—that are extremely hard to obtain in practice—are sufficient, but not necessary. What suffices is a CDT that can be generated efficiently for any 2-D input, whereas for 3-D there may be problems in case of sharp features.

A diagonal material matrix has obvious advantages in Yee-like schemes for electromagnetic propagation. This paper also emphasizes the advantages in solving BVPs. First, the resulting matrix has a reduced fill-in and is an *M*-matrix, which can be efficiently solved with algebraic multigrid solvers and it preserves the discrete maximum principle. Second, the complementary bounds on global parameters obtained by the proposed formulation together with the scalar potential one are quite symmetric with respect to the exact solution, thus the mean of the values obtained by the two methods is extremely accurate. Fig. 5 shows this mean for the MEMS comb drive problem.

References

[1] T. Weiland, "A discretization model for the solution of Maxwell's equations for six-component fields," *Electron. Commun.*, vol. 31, no. 3, pp. 116–120, 1977.
[2] E. Tonti, "On the formal structure of physical theories," Italian National Research Council, Genoa, Italy, Tech. Rep., 1975.
[3] A. Bossavit, *Géométrie de L'électromagnétisme et Éléments Finis*. Paris, France: Hermès-Lavoisier, 2003.
[4] R. Specogna, "Complementary geometric formulations for electrostatics," *Int. J. Numer. Methods Eng.*, vol. 86, no. 8, pp. 1041–1068, 2011.
[5] Z. Ren and X. Xu, "Dual discrete geometric methods in terms of scalar potential on unstructured mesh in electrostatics," *IEEE Trans. Magn.*, vol. 50, no. 2, Feb. 2014, Art. ID 7000704.
[6] K. Yee, "Numerical solution of initial boundary value problems involving Maxwell's equations in isotropic media," *IEEE Trans. Antennas Propag.*, vol. 14, no. 3, pp. 302–307, May 1966.
[7] P. G. Ciarlet, "Discrete maximum principle for finite-difference operators," *Aequationes Math.*, vol. 4, no. 3, pp. 338–352, 1970.
[8] U. van Rienen and T. Weiland, "Triangular discretization method for the evaluation of RF-fields in cylindrically symmetric cavities," *IEEE Trans. Magn.*, vol. 21, no. 6, pp. 2317–2320, Nov. 1985.
[9] M. Marrone, "Computational aspects of cell method in electrodynamics," in *Geometric Methods for Computational Electromagnetics, PIER*, vol. 32, F. L. Teixeira and J. A. Kong, Eds. Cambridge, MA, USA: EMW Publishing, 2002, pp. 317–356.
[10] A. Canova, G. Gruosso, and M. Repetto, "3D electrostatic field solution with dual mesh," *Facta Univ.-Ser., Electron. Energetics*, vol. 15, no. 2, pp. 151–163, 2002.
[11] L. Bernard and L. Pichon, "Generalized finite difference scheme using mainly orthogonal and locally barycentric dual mesh for electromagnetic problems," *Eur. Phys. J. Appl. Phys.*, vol. 52, no. 2, p. 23307, 2010.
[12] X. Xu and Z. Ren, "Investigation on dual finite element method in terms of scalar potentials through interpolations," in *Proc. 16th IEEE Conf. Electromagn. Field Comput. (CEFC)*, 2014.
[13] R. Schuhmann, P. Schmidt, and T. Weiland, "A new Whitney-based material operator for the finite-integration technique on triangular grids," *IEEE Trans. Magn.*, vol. 38, no. 2, pp. 409–412, Mar. 2002.
[14] P. Alotto, A. De Cian, and G. Molinari, "A time-domain 3-D full-Maxwell solver based on the cell method," *IEEE Trans. Magn.*, vol. 42, no. 4, pp. 799–802, Apr. 2006.
[15] B. Delaunay, "Sur la sphère vide," *Izv. Akad. Nauk SSSR, Otdelenie Matematicheskikh i Estestvennykh Nauk*, vol. 7, no. 6, pp. 793–800, 1934.
[16] V. T. Rajan, "Optimality of the Delaunay triangulation in $\mathbb{R}^d$," *Discrete Comput. Geometry*, vol. 12, no. 1, pp. 189–202, 1994.
[17] H. Edelsbrunner and T. S. Tan, "An upper bound for conforming Delaunay triangulations," *Discrete Comput. Geometry*, vol. 10, no. 1, pp. 197–213, 1993.
[18] J. R. Shewchuk, "Delaunay refinement algorithms for triangular mesh generation," *Comput. Geometry*, vol. 22, nos. 1–3, pp. 21–74, 2002.
[19] J. R. Shewchuk, "Triangle: Engineering a 2D quality mesh generator and Delaunay triangulator," in *Proc. Workshop Appl. Comput. Geometry Towards Geometric Eng. (FCRC/WACG)*, 1996, pp. 203–222.
[20] G. Voronoï, "Nouvelles applications des paramètres continus à la théorie des formes quadratiques," *J. Reine Angew. Math.*, vol. 133, pp. 97–102, Jan. 1908.
[21] H. Si, K. Gärtner, and J. Fuhrmann, "Boundary conforming Delaunay mesh generation," *Comput. Math. Math. Phys.*, vol. 50, no. 1, pp. 38–53, 2010.
[22] M. Murphy, D. M. Mount, and C. W. Gable, "A point-placement strategy for conforming Delaunay tetrahedralization," *Int. J. Comput. Geometry Appl.*, vol. 11, no. 6, pp. 669–682, 2001.
[23] D. Cohen-Steiner, E. C. de Verdière, and M. Yvinec, "Conforming Delaunay triangulations in 3D," *Comput. Geometry*, vol. 28, nos. 2–3, pp. 217–233, 2004.
[24] S. E. Pav and N. J. Walkington, "Robust three dimensional Delaunay refinement," in *Proc. 13th Int. Meshing Roundtable*, Sep. 2004, pp. 145–156.
[25] S.-W. Cheng and S.-H. Poon, "Three-dimensional Delaunay mesh generation," *Discrete Comput. Geometry*, vol. 36, no. 3, pp. 419–456, 2006.
[26] R. Specogna, "One stroke complementarity for Poisson-like problems," *IEEE Trans. Magn.*, to be published, doi: 10.1109/TMAG.2014.2358264.